

Linear kinetic Sunyaev-Zel'dovich effect and void models for acceleration

James P. Zibin^{*} and Adam Moss[†]

Department of Physics and Astronomy, University of British Columbia, Vancouver, BC, V6T 1Z1 Canada

(Dated: July 28, 2021)

There has been considerable recent interest in cosmological models in which the current apparent acceleration is due to a very large local underdensity, or *void*, instead of some form of dark energy. Here we examine a new proposal to constrain such models using the linear kinetic Sunyaev-Zel'dovich (kSZ) effect due to structure within the void. The simplified “Hubble bubble” models previously studied appeared to predict far more kSZ power than is actually observed, independently of the details of the initial conditions and evolution of perturbations in such models. We show that the constraining power of the kSZ effect is considerably weakened (though still impressive) under a fully relativistic treatment of the problem, and point out several theoretical ambiguities and observational shortcomings which further qualify the results. Nevertheless, we conclude that a very large class of void models is ruled out by the combination of kSZ and other methods.

PACS numbers: 98.80.Es, 95.36.+x, 98.65.Dx

I. INTRODUCTION

Probably the most surprising cosmological discovery in recent decades has been the unexpected faintness of distant Type Ia supernovae (SNe) (see [1] for a review of the discovery). This has been widely interpreted as evidence for the accelerated expansion of the Universe due to a cosmological constant (or similarly behaving “dark energy”), or due to a modification to general relativity on very large scales.

The standard picture of an accelerating, homogeneous and isotropic Friedmann-Lemaître-Robertson-Walker (FLRW) Universe is now supported by a wide variety of observations in addition to SNe (see [2, 3] for reviews of the evidence). Nevertheless, uncertainty about the fundamental origin of a small cosmological constant has led to considerable effort in studying alternative models in which inhomogeneity plays a key role. The simplest of these, both conceptually and practically, is the idea that an observer in an approximately spherical underdensity, or *void*, which extends to redshift $z \simeq 1$, will observe an *apparent* acceleration due to the inhomogeneity [4–6]. These models dispense with the need for a mysterious dark energy component at the cost of a violation of the Copernican principle, since the observer must be very close to the centre of the void in order to satisfy cosmic microwave background (CMB) dipole constraints [7–10]. Although void models (and others based on inhomogeneity) potentially solve the coincidence problem with the standard Λ FLRW model¹ by linking the appearance of acceleration to the formation of nonlinear structures, they are not free of temporal tuning [11].

Considerable effort has gone into confronting such void

models for acceleration with a variety of different data (see, e.g., the reviews [12, 13] in this focus section). SN data can always be satisfied by choosing the radial profile of a void to match the redshift-luminosity distance relation of Λ FLRW [14]; nevertheless, these data do put crucial constraints on the depth and width of a void. Another class of observations involves the properties of structures within the void, e.g. studies of the baryon acoustic oscillations (BAO) [15, 16]. While potentially very constraining, these approaches are hampered by the difficulty of predicting the evolution of perturbations on LTB backgrounds [17, 18], although in special cases, such as near the centre, the evolution can be followed analytically and strong constraints made [19]. More fundamentally, these approaches are hindered by our ignorance of the initial conditions (ICs) for the perturbations within the void: since the origin of the void itself is unclear, we cannot be sure that the ICs which apply at the radius of last scattering (and are manifest in the CMB) also apply locally.

The primary anisotropies in the CMB contain a wealth of information, and hence their ability to constrain void models has been carefully studied. As first pointed out in [16], as long as the primordial spectrum is close to scale invariant, observations of the CMB temperature anisotropy spectrum can only be satisfied in void models if the *local* expansion rate is so low as to rule the models out. These results were shown to persist when the void is embedded in a spatially curved background [19–21].

The CMB is also expected to contain a variety of secondary anisotropies generated at late times. Galaxy clusters within the void will see very large CMB dipoles and hence are expected to produce substantial anisotropies via the kinetic Sunyaev-Zel'dovich (kSZ) effect [22], as first suggested in [23]. This has been used to put constraints on void models in [24, 25]. Recently, a related approach in which the kSZ anisotropies due to all structure within the void are considered was introduced by Zhang and Stebbins [26] (hereafter ZS10). The authors found that void models predicted far more kSZ power than

^{*}Electronic address: zibin@phas.ubc.ca

[†]Electronic address: adammos@phas.ubc.ca

¹ We refer to the standard cosmological model as Λ FLRW to emphasize its geometry, whereas the more common term “ Λ cold dark matter” (Λ CDM) emphasizes its matter content.

is actually observed at small angular scales, and hence claimed that all such models were ruled out. However, ZS10 employed a simplified non-relativistic void model and did not examine the dependence of the effect on a variety of parameters.

In this work we aim to repeat the analysis of ZS10, but in a fully consistent general relativistic framework. We employ the exact, spherically symmetric pressureless matter solution to Einstein's equations, known as the Lemaître-Tolman-Bondi (LTB) spacetime [27–29]. We assume that the LTB model contains no decaying mode, since we can then maintain the standard picture of an early homogeneous Universe consistent with inflation. We also ignore the possibility of a large, early isocurvature mode between radiation and matter. We assume, with ZS10, that the matter power spectrum today is that of the standard Λ FLRW model, hence bypassing all uncertainty related to the ICs and evolution of perturbations inside the void. However, we show that the question of which *scales* the spectrum is to be evaluated at is not trivial. We confirm that void models which satisfy the SN data overpredict kSZ power, though considerably less so than indicated in ZS10, and point out that there are numerous theoretical ambiguities and observational uncertainties that affect the reliability of kSZ calculations in void models.

We begin in section II with a calculation of the kSZ power in LTB models. We point out that there is considerable ambiguity in relating length scales in LTB and standard Λ FLRW models, but propose a resolution. Next, in section III, we illustrate kSZ spectra and the distribution of power in wave number and redshift space. Section IV presents void model constraints using SN and local Hubble rate data. Section V examines the dependence of the kSZ power on various parameters. We extend our results to a calculation of the Compton y -distortion in section VI. Our conclusions are presented in section VII. The Appendix presents a brief description of our LTB models. Throughout this paper we set $c = 1$ and define the conventional dimensionless Hubble rate h_0 via $H_0 \equiv 100 h_0 \text{ km s}^{-1} \text{ Mpc}^{-1}$.

II. CALCULATING THE LINEAR KINETIC SUNYAEV-ZEL'DOVICH EFFECT

A. Derivation of the kSZ power

The kSZ effect [22] due to Thomson scattering of the CMB from free electrons is conventionally written as

$$\frac{\Delta T(\mathbf{n})}{T} = \int \mathbf{v}(\mathbf{n}, z) \cdot \mathbf{n} [1 + \delta(\mathbf{n}, z)] d\tau, \quad (1)$$

where \mathbf{n} is the line-of-sight direction, $\delta(\mathbf{n}, z) \equiv \delta\rho_e(\mathbf{n}, z)/\rho_e(z)$ is the comoving free electron density perturbation in direction \mathbf{n} and at redshift z , and τ is the optical depth along the line of sight. The quantity $\mathbf{v}(\mathbf{n}, z)$ is the relative velocity between the free electrons and the

CMB rest frame (the frame in which the CMB dipole vanishes) at (\mathbf{n}, z) . A scatterer at (\mathbf{n}, z) will observe a *radial* component of a CMB dipole directly related to the radial component $\beta(\mathbf{n}, z) \equiv \mathbf{v}(\mathbf{n}, z) \cdot \mathbf{n}$.²

In an FLRW background, the dipole $\beta(\mathbf{n}, z)$ vanishes by isotropy. Therefore in realistic models with structure, $\beta(\mathbf{n}, z)$ is a perturbative quantity, corresponding to peculiar velocities. In an inhomogeneous LTB background, on the other hand, the lack of isotropy away from the centre means that the dipole will not generally vanish. Therefore, in a model with structure on top of an LTB background, we can decompose the dipole according to $\beta(\mathbf{n}, z) = \bar{\beta}(z) + \delta\beta(\mathbf{n}, z)$, with the first part due to the LTB background (a very-large-scale “bulk velocity”), and the second part due to the superimposed perturbative structure (peculiar velocities relative to the LTB background). Therefore we can write the kSZ anisotropy as

$$\frac{\Delta T(\mathbf{n})}{T} = \int [\bar{\beta}(z) + \delta\beta(\mathbf{n}, z)][1 + \delta(\mathbf{n}, z)] d\tau \quad (2)$$

(we henceforth drop the bar over $\beta(z)$). We initially assume that the free electron fluctuations match those of the total matter, so that $\delta\rho_e/\rho_e = \delta\rho_m/\rho_m$, but consider the validity of this approximation in section VB. The dipole and density perturbations are evaluated on the light cone, so, e.g.,

$$\delta(\mathbf{n}, z) = \delta(\mathbf{n}, t(z), r(z)) \quad (3)$$

for time coordinate t and radial coordinate r . We will often use the shorthand notation

$$Q(r) = Q(t(z), r(z)) = Q(z) \quad (4)$$

or

$$Q(t) = Q(t(z), r(z)) \quad (5)$$

for quantities $Q(t, r)$ evaluated on the observer's past light cone.

As we mentioned above, in FLRW backgrounds the background dipole vanishes, $\bar{\beta}(z) = 0$. In this case, the linear term in (2), $\int \delta\beta d\tau$, is negligible due to a geometrical cancellation [30]. Therefore the second order term $\int \delta\beta\delta d\tau$ dominates, and the effect in that case is sometimes known as the Ostriker-Vishniac effect [31]. In LTB void models, the term $\int \bar{\beta} d\tau$ contributes only a small monopole³ and hence we will ignore it. We will assume that the term $\int \delta\beta d\tau$ vanishes (or at least that it is subdominant) in LTB models as it does in the FLRW case. Hence we are left with one relevant first order term,

$$\frac{\Delta T(\mathbf{n})}{T} = \int \bar{\beta}(z) \delta(\mathbf{n}, z) d\tau. \quad (6)$$

² In terms of the spherical harmonic coefficients $a_{\ell m}$ to be defined in (13), we have $\beta(\mathbf{n}, z) = \sqrt{3/(4\pi)} a_{10}(\mathbf{n}, z)$, when the polar axis is aligned along \mathbf{n} .

³ However, this term should lead to higher multipole anisotropies in nonspherical voids.

The fact that (6) is *linear* in the fluctuation amplitude leads us to call it the *linear* kSZ effect, after ZS10, and will result in much larger kSZ power in void models than in FLRW models. It is important to stress that the linear kSZ effect is fundamentally different from the nonlinear effect in FLRW models. Because the linear kSZ effect does not contain dipole perturbations (i.e. peculiar velocities), it is independent of the details of the velocity power spectrum. On the other hand, the velocity power is crucial in the calculation of kSZ in FLRW models. The insensitivity to the velocity power removes a significant source of uncertainty in the LTB kSZ calculation, although considerable ambiguities will remain, as we will see.

In order to evaluate the kSZ integral (6), we will wish to perform a harmonic decomposition of the perturbation field $\delta(\mathbf{n}, z)$. To be able to do this, the field should be defined on a flat (or at least constant-curvature) space-like hypersurface. However, flat slices are not natural in general LTB spacetimes: they will not generally be orthogonal to the comoving worldlines, so hypersurfaces of constant proper time will not be of constant curvature. Nevertheless, recalling that we are restricting the LTB models to growing mode profiles, we can bypass this difficulty by relating the perturbation field on the past light cone, $\delta(\mathbf{n}, z)$, to that on some slice t_i , early enough that the LTB spacetime is close to FLRW at that time. We can then perform a decomposition on the early slice. Therefore, we introduce a growth function $D(t)$ to relate the density perturbations at t_i , $\delta_i(\mathbf{n}, r) \equiv \delta(\mathbf{n}, t_i, r)$, to those at some later time via

$$\delta(\mathbf{n}, t(z), r(z)) = D(t(z))\delta_i(\mathbf{n}, r(z)). \quad (7)$$

By virtue of this expression, the coordinate r must be comoving. For the case of linear fluctuations about an FLRW background dominated by dust and cosmological constant at late times, we have the simple relation

$$D(t) = \frac{a(t)}{a(t_i)} \frac{g(t)}{g(t_i)}, \quad (8)$$

Now, substituting (9) and (7), we can write (6) as

$$\frac{\Delta T(\mathbf{n})}{T} = \sqrt{\frac{2}{\pi}} \int dr F(r) D(t(r)) \int dk k \sum_{\ell m} \delta_{i, \ell m}(k) j_\ell(kr) Y_{\ell m}(\mathbf{n}), \quad (10)$$

where

$$F(r) \equiv \beta(r) \frac{d\tau}{dr}. \quad (11)$$

As we mentioned above, this expression for the kSZ anisotropy ignores scale dependence in the perturbation evolution. However, as we will see below, the matter power on nonlinear scales will be crucial to the strength of the kSZ technique in constraining LTB models. Therefore, in order to capture the effect of the nonlinear power, we must promote the growth function to be scale dependent, $D(t) \rightarrow D(t, k)$. With this replacement, (10) becomes

$$\frac{\Delta T(\mathbf{n})}{T} = \sqrt{\frac{2}{\pi}} \int dr F(r) \int dk k D(t(r), k) \sum_{\ell m} \delta_{i, \ell m}(k) j_\ell(kr) Y_{\ell m}(\mathbf{n}). \quad (12)$$

where $a(t)$ is the FLRW scale factor and $g(t)$ the usual growth suppression factor.

It is very important to point out that the relation (7) neglects a couple of significant physical effects. First, in relating the perturbation at some coordinates (\mathbf{n}, t, r) to that on the same comoving worldline at (\mathbf{n}, t_i, r) , it ignores any scale dependence in the evolution. In particular, at late times the nonlinear growth is expected to be greatest on the smallest scales. The second effect is that the scalar perturbation evolution on the LTB background is expected to couple to vector and tensor modes, necessarily coupling different comoving worldlines. However, in the approximation that the coupling to tensors is ignored, it can be shown that the evolution satisfies a relation similar to (7) [17]. More importantly, as mentioned in the [Introduction](#), we will not attempt a description of the perturbation ICs and evolution in this work; instead, we will assume that the actual matter power spectrum on the light cone is close to that of the standard Λ FLRW model. Therefore, we will consider it reasonable to ignore this latter effect. On the other hand, it will be necessary to deal with the former effect in an ad hoc manner by introducing scale dependence below.

The LTB growing mode assumption allows us to expand the field $\delta_i(\mathbf{n}, r)$ in spherical harmonic functions, $Y_{\ell m}(\mathbf{n})$, and spherical Bessel functions of the first kind, $j_\ell(kr)$, according to

$$\delta_i(\mathbf{n}, r) = \sqrt{\frac{2}{\pi}} \int dk k \sum_{\ell m} \delta_{i, \ell m}(k) j_\ell(kr) Y_{\ell m}(\mathbf{n}), \quad (9)$$

where k is the wave number. It is important to stress the meaning of the quantities r and k here: the radial comoving coordinate r must be proportional to *proper* distance at t_i (at least at background level, on the nearly FLRW background), and the wave number k is similarly proportional to proper wave number, in order that the harmonic decomposition be valid.

To avoid this ad hoc procedure would require developing the theory of perturbations on LTB backgrounds. While some progress has been made in the linear case [17, 18], the nonlinear case has not yet been addressed. However, although strictly the growth function $D(t, k)$ is ill-defined since we cannot perform a harmonic decomposition at late times, this procedure might be justified in that it may be possible to consider such a decomposition valid on the very small scales (much smaller than the LTB curvature scale) relevant to the kSZ effect. This leads to our first major caveat: our result will likely be invalid on the largest angular scales, and the degree of accuracy will be uncertain even on small scales.

Next we can calculate the spherical harmonic coefficients of the observed temperature field,

$$a_{\ell m} \equiv \int \frac{\Delta T(\mathbf{n})}{T} Y_{\ell m}^*(\mathbf{n}) d\Omega \quad (13)$$

$$= \sqrt{\frac{2}{\pi}} \int dr F(r) \int dk k D(r, k) \delta_{i, \ell m}(k) j_{\ell}(kr). \quad (14)$$

Finally, the kSZ power at multipole ℓ is given by

$$C_{\ell} \equiv \langle a_{\ell m} a_{\ell m}^* \rangle \quad (15)$$

$$= 4\pi \int \frac{dk}{k} \mathcal{P}_{\delta_i}(k) \left(\int dr F(r) D(r, k) j_{\ell}(kr) \right)^2. \quad (16)$$

In deriving this final expression, we have used the defining relation

$$\langle \delta_{i, \ell m}(k) \delta_{i, \ell' m'}^*(k') \rangle = \frac{2\pi^2}{k^3} \mathcal{P}_{\delta_i}(k) \delta(k - k') \delta_{\ell \ell'} \delta_{m m'} \quad (17)$$

for the power spectrum $\mathcal{P}_{\delta_i}(k)$ of Gaussian random matter field $\delta_i(\mathbf{n}, r)$. The spectrum $\mathcal{P}_{\delta_i}(k)$ is well defined since a harmonic decomposition is possible at t_i , when the spacetime is near FLRW.

Equation (16) provides a general expression for the kSZ power on LTB backgrounds, subject to the major caveat regarding the ambiguity of defining the growth factor $D(r, k)$. The factor $F(r)$ in the integrand will depend on the particular radial LTB profile chosen. It can be written

$$F(r) = \beta(r) \frac{d\tau}{dz} \frac{dz}{dr}, \quad (18)$$

where

$$\frac{d\tau}{dz} = \frac{\sigma_T f_b (2 - Y_{\text{He}}) \rho_m(z)}{2m_p (1 + z) H_{\parallel}(z)} \quad (19)$$

and

$$\frac{dz}{dr} = (1 + z) H_{\parallel}(z) \frac{Y'}{\sqrt{1 - K}}. \quad (20)$$

Here σ_T is the Thomson cross section, $f_b \equiv \rho_b / \rho_m$ is the baryon fraction, Y_{He} is the helium mass fraction, m_p is the proton mass, and the remaining LTB functions

are defined in the [Appendix](#). This expression applies after reionization, when we have assumed that the baryonic matter is completely ionized. We use the value $Y_{\text{He}} = 0.24$ throughout this work, and nominally set $f_b = 0.168$, as implied by CMB observations [32]. As we discuss in detail in section V A, it is likely that this standard value of baryon fraction should be modified locally in void models, leading to considerable uncertainty in our kSZ predictions.

B. The matter power spectrum

After the LTB profile is specified, the remaining quantities required to calculate the kSZ power are the matter power spectrum $\mathcal{P}_{\delta_i}(k)$ and the growth function $D(r, k)$. As explained above, we do not attempt to calculate these quantities from ICs; rather, we begin by assuming that the actual matter power along our past light cone matches that of the standard Λ FLRW model. Later we will consider the effect of relaxing this assumption. However, implementing even this simple prescription for the matter power is far from trivial. First, as already mentioned in section II A, it is not clear how to define a power spectrum at late times when a harmonic decomposition is not possible. But there is a second important reason: the wave numbers k with respect to which the power spectra are specified have different meanings and behaviours in LTB and FLRW models. Since the matter power spectrum can depend sensitively on scale, this will lead to a further significant ambiguity in specifying the matter power.

To see this, note first of all that, for FLRW models, the power spectrum on the past light cone, $\mathcal{P}_{\delta}(k, z)$, is usually specified in terms of *comoving* wave number k (or k/h_0), which is equivalent to *proper* wave number today. In general, perturbation modes in LTB and FLRW models with identical proper wave numbers today will not share identical proper wave numbers on the past light cone, due to the very different background evolution of the two models. (Recall that the LTB and standard Λ FLRW background evolutions differ at *zeroth* order.) Therefore it is certainly incorrect to state that the LTB model should share the same $\mathcal{P}_{\delta}(k, z)$ at the same proper wave number *today* as the standard Λ FLRW model.

However, it is *also* generally incorrect to require that the power $\mathcal{P}_{\delta}(k, z)$ be the same in both models at the same proper k specified at the *same redshift* z on the past light cone. The reason is that what is actually observed in galaxy surveys is not proper wave numbers at some z , but rather angular and redshift separations. A pair of galaxies with the same proper separation at the same z in LTB and FLRW models will generally be observed with very different angular and redshift separations in the two models, again due to the different background geometry.

Therefore, what we require is that the LTB model has the same matter power on the same angular and redshift scales, at the same z , as the standard Λ FLRW model. In

any model, for a mode oriented perpendicular to the line of sight with *proper* wave number k_\perp at redshift z , the corresponding angular scale on the sky is

$$\Delta\theta = \frac{\alpha}{k_\perp(z)d_A(z)}, \quad (21)$$

where $d_A(z)$ is the angular diameter distance to z , measured as a *proper* distance at z , and α is a constant (independent of the model) of order unity. Therefore, if the two models are to share the same power at the same angular scales, they must have the same power at proper wave numbers related by

$$k_\perp^{\text{LTB}}(z) = k_\perp^\Lambda(z) \frac{d_A^\Lambda(z)}{d_A^{\text{LTB}}(z)}. \quad (22)$$

In practice, if the LTB model is to fit the Type Ia supernova data and measurements of the local Hubble rate, then $d_A^{\text{LTB}}(z)$ must be similar to $d_A^\Lambda(z)$, at least out to $z \simeq 1$, and hence a first approximation would be to set $k_\perp^{\text{LTB}}(z) = k_\perp^\Lambda(z)$.

Similarly, if the two models are to share the same power at the same redshift scales, they must have the same power at proper wave numbers related by

$$k_\parallel^{\text{LTB}}(z) = k_\parallel^\Lambda(z) \frac{H_\parallel^{\text{LTB}}(z)}{H^\Lambda(z)}. \quad (23)$$

This leads directly to a fundamental problem: generically, we will have $k_\perp^{\text{LTB}}(z) \neq k_\parallel^{\text{LTB}}(z)$, when $k_\perp^\Lambda(z) = k_\parallel^\Lambda(z)$, due to the background geometry of the LTB models.⁴ This means that there is no unique scale in Λ FLRW corresponding to a particular scale in the LTB model, and vice versa. (Indeed, this discrepancy between angular and redshift scales in the two models results in the strength of the radial BAO scale in constraining LTB models [16, 19].)

To patch over this problem, we define an “isotropized” version of the relation between wave numbers in the two models by

$$k^\Lambda(z) \equiv \left[(k_\perp^\Lambda(z))^2 k_\parallel^\Lambda(z) \right]^{1/3} \quad (24)$$

$$= \left[\left(k_\perp^{\text{LTB}}(z) \frac{d_A^{\text{LTB}}(z)}{d_A^\Lambda(z)} \right)^2 k_\parallel^{\text{LTB}}(z) \frac{H^\Lambda(z)}{H_\parallel^{\text{LTB}}(z)} \right]^{1/3} \quad (25)$$

This relation weights the transverse relation more heavily than the radial one, since there are twice as many transverse dimensions. It is important to stress that the particular form of this relation we have chosen is still largely arbitrary. [This notion of an isotropized scale is

akin to the isotropized distance measure often used in the literature on BAO observations (e.g. [33]). Our final statement, then, is that the LTB and Λ FLRW models must share the same matter power on scales related by (25). The ambiguity in this relation leads to our second major caveat: uncertainty in the k scales, together with the sensitivity of the matter power to k in standard spectra, will lead to further uncertainty in the calculated kSZ power.

The evolution of proper wave numbers in the radial and transverse directions in the LTB model is straightforward to specify. For a mode of proper wave number $k(t_i)$ specified at the time t_i early enough that the space-time is near FLRW (and hence the power spectrum is presumably isotropic), we have

$$k_\perp(t, r) = k(t_i, r) \frac{Y(t_i, r)}{Y(t, r)}, \quad k_\parallel(t, r) = k(t_i, r) \frac{Y'(t_i, r)}{Y'(t, r)}. \quad (26)$$

We stress again that our inability to perform proper harmonic decompositions of fields at late times implies that we must interpret relations of this sort loosely.

Recall that the general expression for kSZ power (16) involves an integral over *proper* k at t_i . To determine the matter power on the corresponding scale, we first use (26) to relate the k values at t_i to those on the light cone in the LTB model. We then use (25) to calculate the corresponding scale in the standard Λ FLRW model, using the fitting function of [34] and the WMAP7 best-fit parameters [32] to evaluate $d_A^\Lambda(z)$ and $H^\Lambda(z)$. The Λ FLRW power can be calculated using any of several public codes; we used CAMB [35], which optionally includes nonlinear power with a Halofit calculation [36]. Our matter spectrum used the normalization provided by CMB observations [32], $\sigma_8 = 0.81$, where σ_8 is the linear amplitude on a scale of $8/h_0$ Mpc. As we discuss in section V A, however, there is considerable ambiguity over this choice in the context of LTB models. Finally, note that (25) becomes ill-defined when $H_\parallel^{\text{LTB}}(z) \leq 0$. This does in fact happen for the very deepest voids, leading to multi-valued distance-redshift relations [37]. Therefore our kSZ calculations will not be valid in the multi-valued regime.

C. The Limber approximation

We can significantly simplify the kSZ power expression (16) using the so-called Limber approximation [38]. This approximation is purely mathematical, as opposed to the physical approximations discussed previously. To employ it, we substitute

$$j_\ell(kr) \simeq \sqrt{\frac{\pi}{2\ell+1}} \delta(\ell+1/2 - kr) \quad (27)$$

in (16). This substitution will be accurate to $\mathcal{O}(1/\ell^2)$ when the integrand $F(r)D(r, k)$ is slowly varying on the scale of the Bessel oscillations [39]. The result for the kSZ power is

⁴ This same model dependence in the meaning of $\mathcal{P}_\delta(k, z)$ will also be present when comparing different *FLRW* models, although to a lesser degree than with LTB models.

$$C_\ell \simeq \frac{4\pi^2}{2\ell+1} \int \frac{dk}{k} F^2 \left(\frac{2\ell+1}{2k} \right) D^2 \left(\frac{2\ell+1}{2k}, k \right) \frac{\mathcal{P}_{\delta_i}(k)}{k^2} \quad (28)$$

$$= \frac{16\pi^2}{(2\ell+1)^3} \int dr r F^2(r) D^2 \left(r, \frac{2\ell+1}{2r} \right) \mathcal{P}_{\delta_i} \left(\frac{2\ell+1}{2r} \right). \quad (29)$$

If we attempt to define a matter power spectrum on the light cone by $\mathcal{P}_\delta(k, z) = D^2(z, k) \mathcal{P}_{\delta_i}(k)$, then (29) becomes

$$C_\ell \simeq \frac{16\pi^2}{(2\ell+1)^3} \int dr r F^2(r) \mathcal{P}_\delta \left(\frac{2\ell+1}{2r}, z(r) \right). \quad (30)$$

Note that all k values in these expressions are proper wave numbers evaluated at t_i . To specify the standard Λ FLRW matter spectrum, we must relate these early time k values to corresponding scales in the Λ FLRW model using the procedure described in section II B.

Equation (30) apparently has a simple interpretation as an integration down the past light cone of a weighted local matter power spectrum. However, it is important to stress that the interpretation of the late time spectrum $\mathcal{P}_\delta(k, z)$ is highly ambiguous, as discussed in sections II A and II B. The same replacement of $\mathcal{P}_{\delta_i}(k)$ with $\mathcal{P}_\delta(k, z)$ cannot be made with the exact expression for kSZ power, (16), and hence neither can such a simple interpretation be made. Note that (30) is equivalent to the corresponding expression in ZS10, up to $\mathcal{O}(1/\ell)$. The specific ℓ -dependent prefactors in (30) ensure that it is accurate to $\mathcal{O}(1/\ell^2)$.

The Limber approximation provides a significant advantage to numerical computations, especially if a large region of parameter space is to be explored. Therefore it is important to check its accuracy. Figure 1 presents the relative error between the Limber calculation of kSZ power using (29) and the exact calculation using (16),

$$\frac{\Delta C_\ell}{C_\ell^{\text{exact}}} \equiv \frac{C_\ell^{\text{Limber}} - C_\ell^{\text{exact}}}{C_\ell^{\text{exact}}}, \quad (31)$$

for the fiducial LTB model (which is described below). The Limber approximation can be seen to be very accurate, to better than a tenth of a percent, over a wide range of angular scales. This was expected, as the integrand $F(r)D(r, k)$ in (16) varies slowly over the width of a void.⁵ Henceforth, all calculations will be performed using the Limber approximation, (29), or equivalently (30).

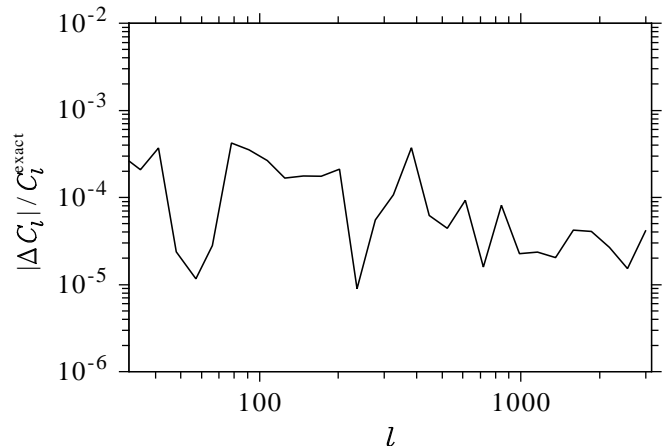


FIG. 1: The relative error of the Limber approximation given by (29), C_ℓ^{Limber} , with respect to the exact kSZ power given by (16), C_ℓ^{exact} . $\Delta C_\ell \equiv C_\ell^{\text{Limber}} - C_\ell^{\text{exact}}$. Results are presented for the fiducial LTB model.

III. BEHAVIOUR OF KSZ POWER IN VOID MODELS

With the formalism for calculating the kSZ power in place, we can now proceed to calculate spectra for specific LTB models, and to investigate where in k and z space the kSZ power is sourced. First, the LTB background must be specified. This entails the specification of a radial profile $K(r)$, together with the *local* Hubble rate at the centre today, H_0 . Our *fiducial profile* for $K(r)$ is defined in the Appendix. Our *fiducial model* is further specified by the parameters $\Omega_{m,0}^{\text{loc}} = 0.2$, $z_L = 0.5$, and $h_0 = 0.71$, where $\Omega_{m,0}^{\text{loc}} \equiv \Omega_m^{\text{loc}}(z=0)$ is the local density parameter at the centre today, and z_L is a measure of the width of the profile in redshift. As we will see in section IV, the fiducial model is a very good fit to the supernova data.

Then the kSZ power can be calculated using the Limber expressions (29) or (30). Importantly, in evaluating the function $F(r)$ using expressions (18) to (20), all background quantities must be evaluated consistently using the specified LTB background. The dipole $\beta(r(z))$ is also calculated consistently in the LTB model by propagating past-directed null rays radially inwards and outwards from the point $(t(z), r(z))$ on the past light cone of the central observer to an early time, and comparing the resulting redshifts as described in [19]. The matter

⁵ A more rapidly varying LTB profile might result in a less accurate Limber approximation.

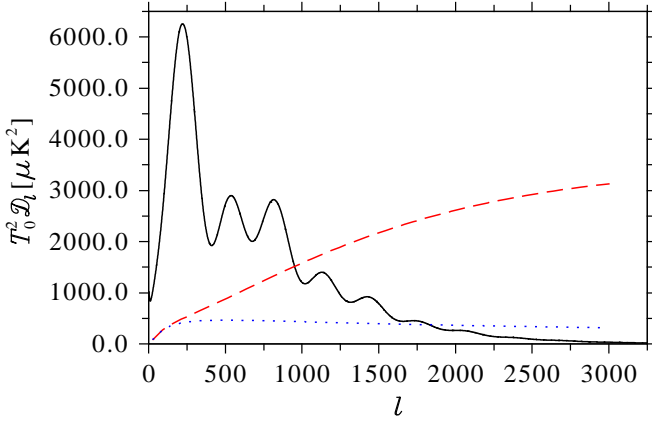


FIG. 2: The kSZ power calculated in the Limber approximation using the Halofit nonlinear matter power (dashed, red curve) and linear power (dotted, blue curve), compared with the temperature anisotropy power in the standard Λ FLRW model (solid, black curve). Results are presented for the fiducial LTB model.

power spectrum in the LTB model is assumed to match that of the standard Λ FLRW model, and is calculated as described in section II B.

A comparison of the kSZ power spectrum calculated for the fiducial LTB model with the temperature anisotropy power in the standard Λ FLRW model is presented in figure 2. The quantities plotted are the conventionally scaled power spectra,

$$\mathcal{D}_\ell \equiv \frac{\ell(\ell+1)C_\ell}{2\pi}. \quad (32)$$

Figure 2 shows the kSZ power calculated using both the nonlinear (Halofit) matter power as well as the corresponding linear spectrum. Nonlinearities in perturbation evolution enhance the matter power on small scales. For the fiducial LTB model and the nonlinear matter power, the kSZ power is found to dominate over the standard temperature anisotropies for $\ell \gtrsim 1000$. Clearly the presence of such a large kSZ component would result in a total anisotropy spectrum drastically different from that actually observed. Although the kSZ power is reduced considerably in the linear matter power case, it still exceeds the standard temperature anisotropies by a large factor for the largest multipoles. While the fiducial model would therefore appear to be immediately ruled out, we will see in section V A that the kSZ power depends sensitively on several parameters.

Figure 2 suggests that the nonlinear matter power on small scales is the main source of the apparently very strong constraint that the kSZ can provide on void models. We can examine this more explicitly by plotting derivatives of the kSZ power. Figure 3 shows the derivative with respect to redshift,

$$\frac{d\mathcal{D}_\ell}{dz} = \frac{8\pi\ell(\ell+1)}{(2\ell+1)^3} \frac{dr}{dz} r F^2(r) \mathcal{P}_\delta \left(\frac{2\ell+1}{2r}, z(r) \right). \quad (33)$$

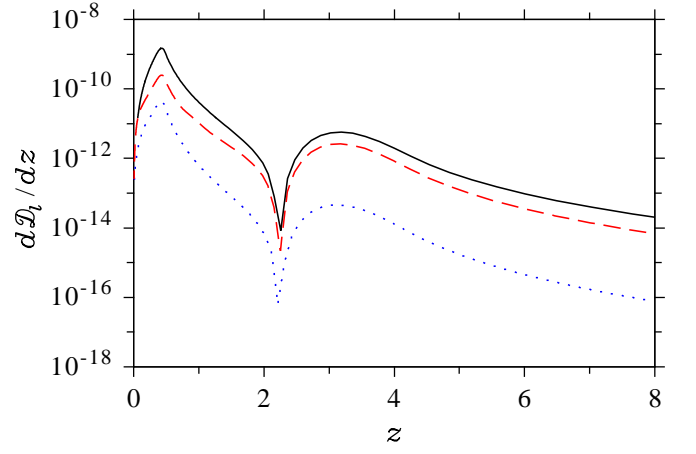


FIG. 3: The derivative of the kSZ power with respect to redshift, calculated in the Limber approximation using the Halofit nonlinear power for three multipoles: $\ell = 30$ (dotted, blue curve), $\ell = 300$ (dashed, red curve), and $\ell = 3000$ (solid, black curve). Results are presented for the fiducial LTB model.

In words, it shows how the contributions to the total power at various distances along the line of sight are distributed. The figure shows that, essentially independently of ℓ , most of the kSZ power originates at redshifts $z \simeq 0.5$, i.e. near the edge of the void for the fiducial model which extends to $z_L = 0.5$. The redshift distribution of the kSZ power is largely determined by the dipole function, $\beta(z)$. Indeed, the dipole peaks near $z = z_L$ and exhibits a zero at $z \simeq 2$ which is visible in figure 3.

Figure 4 shows the derivative of kSZ power with respect to logarithmic k interval,

$$\frac{d\mathcal{D}_\ell}{d \ln k} = \frac{2\pi\ell(\ell+1)}{2\ell+1} F^2 \left(\frac{2\ell+1}{2k} \right) \frac{\mathcal{P}_\delta(k, z)}{k^2}, \quad (34)$$

for both the nonlinear and linear matter power spectrum. That is, it shows how the contributions to the kSZ power from different length scales are distributed. Importantly, the distributions are plotted with respect to the scale k^Λ , calculated as described in section II B (and measured as a proper wave number today). This is the scale that we would conclude a feature lies at if we mistakenly assumed that the Λ FLRW model was correct, when actually the specified LTB model was correct.

As expected from the relation (21), figure 4 shows that the wave numbers sourcing the kSZ power scale in inverse proportion to the angular scale examined on the sky. In addition, it is clear that the length scales sourcing the most powerful part of the kSZ spectrum, near $\ell \simeq 3000$, are strongly nonlinear. Importantly, the figure also shows that the length scales we would infer to make the largest contribution to the high- ℓ kSZ effect are very small: for $\ell = 3000$, the corresponding length scales are roughly 1/3 Mpc. We will discuss the significance of these small scales in section V B.

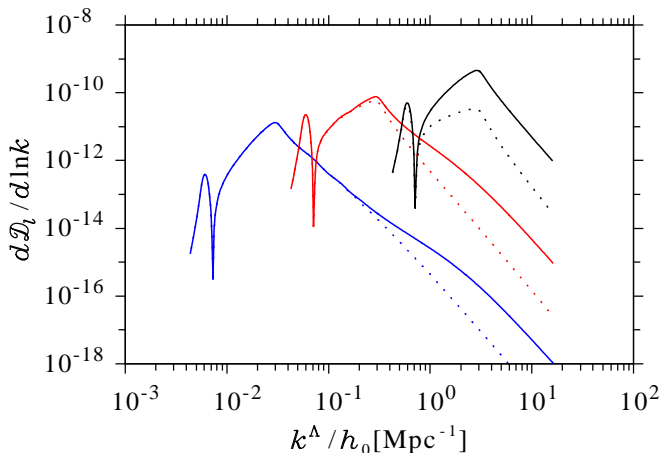


FIG. 4: The derivative of the kSZ power with respect to wave number, calculated in the Limber approximation using the Halofit nonlinear power (top, solid curve of each pair) and linear power (lower, dotted curves). Results are shown for three multipoles: $\ell = 30$ (leftmost, blue pair of curves), $\ell = 300$ (central, red curves), and $\ell = 3000$ (rightmost, black curves). The distributions are plotted with respect to the scale k^Λ/h_0 , calculated as described in section II B, and measured as a proper wave number today. Results are presented for the fiducial LTB model.

IV. CONSTRAINTS ON VOID MODELS

The results of the previous section show that LTB models can potentially exhibit very high kSZ power. In order to determine whether *viable* void models predict too much kSZ power, we must select models which fit other observations. For our analysis we used the *minimal* amount of data required to fix the void profile, and hence obtained the most independent kSZ constraints possible. To do this we used redshift-magnitude measurements of Type Ia SNe from the Union2 compilation [40], consisting of 557 SNe in the range $z = 0.015$ – 1.4 . In our fitting we adopted the standard procedure of marginalizing over the unknown absolute magnitude, which is equivalent to marginalizing over H_0 . A further input is therefore a *local* estimate of H_0 (i.e. for $z \lesssim 0.1$), which is essentially free of any assumptions regarding the cosmological model. For this we used a prior of $h_0 = 0.72 \pm 0.08$ from the Hubble Space Telescope (HST) Key Project [41]. Since our choice of prior has a larger error bar than the more recent measurements in [42, 43], it is more conservative. Note that the SN data are not model independent; instead, they assume a standard Λ FLRW background (e.g., see the discussion in [44]). This will result in further uncertainty in the kSZ power, considering the strong sensitivity of the power to the void width which we will explicate in section V A.

In our previous analyses, we found that much lower values of the local Hubble rate ($h_0 \simeq 0.45$) were required for void models to fit the CMB primary anisotropies, assuming a near-power-law primordial spectrum [16, 19].

Although such low values of H_0 are in severe conflict with the local measurements in [41–43], this tension might in principle be circumvented by substantial fine tuning of the primordial spectrum, allowing for higher values of H_0 . For this reason we chose a prior on H_0 which is consistent with local observations, and we did not include the CMB primaries in our constraints. Another reason we excluded CMB primaries is that, as figure 2 shows, a large linear kSZ component will substantially modify the observed anisotropies over a wide range of scales.

We used COSMOMC [45] to generate Markov-Chain-Monte-Carlo chains to estimate confidence limits. The LTB profile we used was the fiducial profile defined in the Appendix. Three parameters were varied: the void width L and depth K_0 , along with H_0 . For each sample of the chain we computed several derived parameters: the redshift to $r = L$, z_L , the central matter density parameter, $\Omega_{m,0}^{\text{loc}}$, and the kSZ power, \mathcal{D}_ℓ , at $\ell = 2500, 3000, 3500, 4000$, and 4500 . As in our previous analyses we applied a conservative prior of $\Omega_{m,0}^{\text{loc}} > 0.1$ [46, 47]. Deeper voids, with $\Omega_{m,0}^{\text{loc}} < 0.1$, must be correspondingly wider to fit the SN data and hence have the largest kSZ power (as we will see in figure 6). Hence the deepest voids are most strongly ruled out by the kSZ constraint. We also applied a prior of $T_0^2 \mathcal{D}_\ell < 10\,000 \mu\text{K}^2$, since such models would already be excluded at high significance by small-scale CMB experiments such as ACBAR [48]. Since we did not use primary CMB data, which fixes the baryon fraction f_b (at least at the radius of last scattering), we needed to choose a (local) value; we set the fiducial value of $f_b = 0.168$ for the kSZ calculation. Similarly, we set the fiducial value of $\sigma_8 = 0.81$ for the matter power amplitude today. The validity of these assumptions is discussed in the next section.

The best-fit model has a total $\chi^2 = 539$, and therefore a goodness-of-fit comparable to Λ FLRW and the void models in our previous work. In figure 5 we show a histogram of the kSZ power from the chains at various ℓ values. Each distribution is similar over the ℓ range we consider, and hence lower limits on the kSZ power are largely independent of ℓ . The maximum-likelihood value is approximately $2500 \mu\text{K}^2$, with an extended tail due to deeper, wider void profiles. Asymmetric distributions make estimating confidence limits (from counting samples in the histogram) dependent on the tail, but we have checked the robustness of our constraints by also excluding samples with $T_0^2 \mathcal{D}_\ell > 5000 \mu\text{K}^2$. The 2σ lower limit on the kSZ power at $\ell = 3000$ is reduced from $1630 \mu\text{K}^2$ to $1440 \mu\text{K}^2$ when applying this constraint. We take the lower (and more conservative) limit as our baseline value to compare with recent CMB observations on very small scales from the South Pole Telescope (SPT) [49, 50] and the Atacama Cosmology Telescope (ACT) [51]. In figure 6 we show the 1, 2, and 3σ confidence levels in the z_L – $\Omega_{m,0}^{\text{loc}}$ plane. Note that our fiducial model, with $z_L = 0.5$ and $\Omega_{m,0}^{\text{loc}} = 0.2$, is very close to the best fit model.

Single frequency bandpowers from the 150 GHz and 148 GHz channels of SPT and ACT limit the *total*

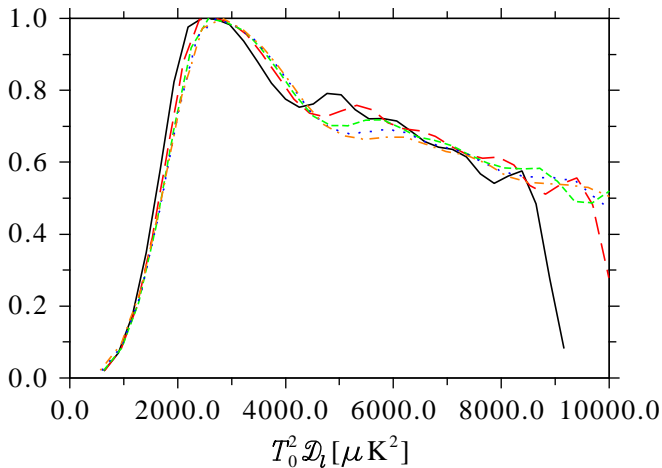


FIG. 5: Histograms of the kSZ power, calculated in the Limber approximation using the Halofit nonlinear power for five multipoles: $\ell = 2500$ (solid, black curve), $\ell = 3000$ (long dashed, red curve), $\ell = 3500$ (short dashed, green curve), $\ell = 4000$ (dotted, blue curve), and $\ell = 4500$ (dot-dashed, orange curve). Results are presented for the fiducial LTB profile, fitted to the Union2 SN data, and using the HST prior of $h_0 = 0.72 \pm 0.08$. Each curve is normalized to unity at its maximum.

power (including primary CMB, point sources, thermal, and kinetic SZ) at $\ell = 3000$ to $\lesssim 50 \mu\text{K}^2$. While both SPT and ACT also present considerably tighter upper limits on the kinetic SZ component itself (and these limits were used in ZS10), such limits are model dependent. This is because the contribution of primary CMB in particular may be quite different in LTB models than in Λ FLRW, recalling that the CMB and H_0 cannot be simultaneously fit without substantially modifying the primordial spectrum. Therefore we consider the SPT and ACT total power to be a conservative upper limit to the kSZ power from voids.⁶ Even taking this conservative approach, the predicted kSZ signal is at least a factor of roughly 30 higher than the observational upper limits, and hence rules out void models which fit the SN data at high significance when the fiducial parameters are assumed.

V. ROBUSTNESS OF KSZ CONSTRAINTS

A. Parameter dependencies

Although the results in section IV suggest that the kSZ anisotropy power is large enough to immediately rule out

⁶ The total powers will almost certainly be overestimates of the kSZ component, since they include a frequency-dependent component presumably due to point sources.

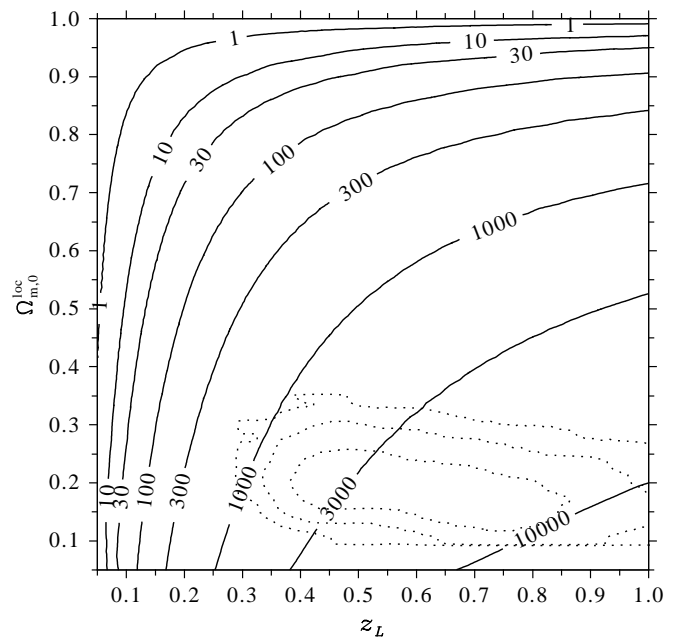


FIG. 6: Solid contours are the kSZ power, $T_0^2 \mathcal{D}_{3000}$ (in μK^2), calculated in the Limber approximation using the Halofit matter power, as a function of central matter density parameter, $\Omega_{m,0}^{\text{loc}}$, and a measure of the width of the void, z_L . Results are presented for the fiducial LTB profile with $h_0 = 0.71$. Dotted contours are the 1, 2, and 3σ confidence levels from the SN data, which used the HST prior of $h_0 = 0.72 \pm 0.08$.

void models for acceleration, it is important to examine the robustness of the kSZ power as a test of homogeneity. In particular, how sensitive are the predictions to various model parameters? This was already addressed to some extent implicitly in section IV, where the LTB profile (width and depth), as well as local Hubble rate, were varied. In this section we will illustrate these dependencies explicitly, and examine the effects of the remaining parameters.

Figure 6 shows the kSZ power for $\ell = 3000$ as a function of a measure of the width of the void, z_L , and the depth of the void as measured by the central density parameter, $\Omega_{m,0}^{\text{loc}}$. The LTB profile used was the fiducial profile, with local Hubble rate $h_0 = 0.71$. Superimposed on figure 6 are the 1, 2, and 3σ confidence levels from the Union2 SN data calculated in section IV. The kSZ power is seen to be a very sensitive function of the void width, varying by roughly a decade over the region allowed by the SNe. Note that, for the fiducial profile, the multi-valued region of parameter space (for which $H_{\parallel}(z) \leq 0$) occurs only for the deepest voids, with $\Omega_{m,0}^{\text{loc}} < 0.05$. Therefore, as noted in section IIB, the kSZ calculation is not valid in this regime and we do not plot it in figure 6. (The excluded shell-crossing region occurs for even deeper voids than the multi-valued models.)

We can understand the general forms of the parameter dependencies illustrated in figure 6 quite easily. For

fixed void width z_L (and fixed H_0), the kSZ power increases as $\Omega_{m,0}^{\text{loc}}$ decreases from unity. This is mainly due to the dipole factor β^2 in the expression for the kSZ, (29). Inside the void, we can define an effective curvature parameter by $\Omega_K^{\text{eff}} \equiv 1 - \Omega_{m,0}^{\text{loc}}$. Then, for a growing mode background solution, we expect $\Omega_{K,0}^{\text{eff}} \propto \delta H/H$, where δH is some measure of the perturbation in expansion rate inside the void relative to the outside [17]. Finally, we expect the dipole at fixed redshift to be proportional to the expansion perturbation,

$$\beta \simeq D\delta H, \quad (35)$$

where D is some proper distance measure [52]. Combining these relations we find

$$C_\ell \propto \beta^2(z_L) \propto (1 - \Omega_{m,0}^{\text{loc}})^2. \quad (36)$$

Although there are considerable ambiguities in defining most of the quantities used to derive this relationship, it is satisfied reasonably well by the numerical results of figure 6.

Next, for fixed $\Omega_{m,0}^{\text{loc}}$ (and fixed H_0), figure 6 shows that the kSZ power grows rapidly with increasing void width z_L . Using the relation (35), we have $\beta^2(r) \propto r^2$, since coordinate r will be approximately proportional to a proper distance measure. Then, ignoring the scale dependence of the matter power spectrum, the kSZ power expression (29) implies

$$C_\ell \propto \int_0^L r^3 dr \propto L^4 \propto z_L^4, \quad (37)$$

for sufficiently small z_L . Again, this relation is indeed roughly satisfied by the numerical results.

Figure 7 illustrates the effect of varying the local Hubble rate, H_0 , while keeping the LTB depth (as measured by $\Omega_{m,0}^{\text{loc}}$) fixed. Larger H_0 leads to larger kSZ power, and this dependence is due to a combination of background factors in the relations (18) to (20), together with the scale dependence of the matter power. The variation in power over our chosen prior range of $h_0 = 0.72 \pm 0.08$ [41] is not large, and of course the variation is considerably smaller over the range of the newer measurement, $h_0 = 0.738 \pm 0.024$ [43].

The remaining parameters that affect the kSZ anisotropy power are the linear matter power amplitude today, σ_8 , conventionally expressed on a scale of $8/h_0$ Mpc, and the baryon fraction f_b . The fluctuation amplitude could also be expressed in terms of the primordial perturbation amplitude, although in our approach of specifying the matter power at late times rather than evolving perturbation ICs, the parameter σ_8 is more natural. If the fluctuations were *linear*, the kSZ power would simply scale as σ_8^2 . However, in the nonlinear regime relevant to the kSZ effect for high ℓ , we expect [53]⁷

$$C_\ell \propto \mathcal{P}_\delta \propto \sigma_8^{2-3}. \quad (38)$$

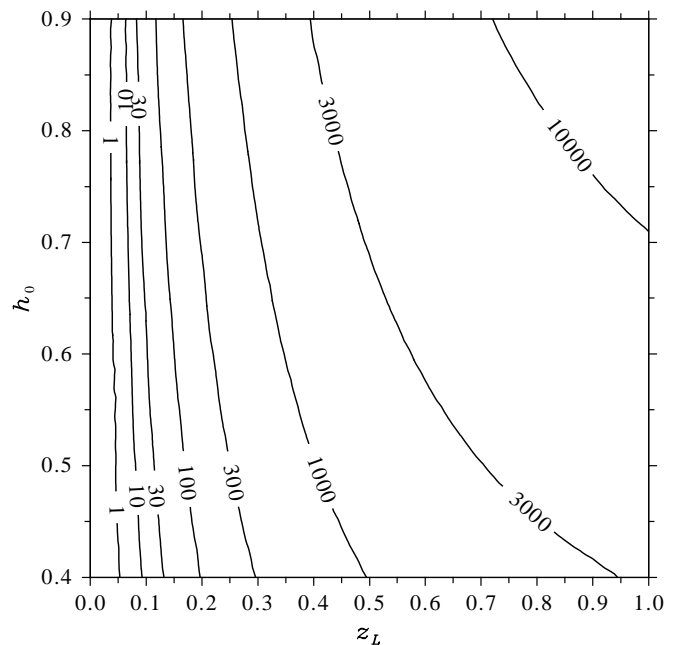


FIG. 7: The kSZ power, $T_0^2 \mathcal{D}_{3000}$ (in μK^2), calculated in the Limber approximation using the Halofit matter power, as a function of local Hubble rate, H_0 , and a measure of the width of the void, z_L . Results are presented for the fiducial LTB profile with $\Omega_{m,0}^{\text{loc}} = 0.2$.

This means that, e.g., an uncertainty of 30% in σ_8 would lead to an uncertainty in the kSZ power of roughly a factor of two.

Of course, observations of the CMB are usually considered to constrain σ_8 very tightly, to a few percent [32]. But this is based on the assumption of homogeneity: void models, on the other hand, contain an extremely large inhomogeneity of mysterious origin, and hence there is no necessary link between the perturbation amplitude locally and that at the last scattering radius. In addition, as mentioned in the Introduction, if we are to satisfy local measurements of H_0 , the primordial spectrum must be modified substantially [16, 19], further clouding the connection between the local and CMB amplitudes. *Local* measurements of σ_8 (or, more precisely, measurements at $z \simeq 0.5$) are what we need to test void models via the kSZ effect; unfortunately, they are considerably more uncertain than those based on the CMB. For example, measurements based on weak lensing (e.g., [54]) constrain only a combination of σ_8 and Ω_m . Extracting constraints on σ_8 from these results would likely be strongly model dependent. Recalling that our calculations have used the standard CMB-based value, $\sigma_8 = 0.81$ [32], we

⁷ For the ordinary (nonlinear) kSZ effect in standard AFLRW mod-

els, the kSZ power scales like an even larger power of σ_8 , since the same amplitude also determines the velocity perturbation spectrum [53].

can expect the uncertain local matter normalization to add significant ambiguity to our calculations.

The final parameter determining the kSZ power is the baryon fraction f_b . This affects the kSZ via the background optical depth, which is related to the background electron density (assumed equal to the baryon density) through (19). A *constant* baryon fraction affects the kSZ power through the simple scaling

$$C_\ell \propto f_b^2. \quad (39)$$

As was the case with the matter power amplitude, constraints on f_b from the CMB will not generally be applicable in an inhomogeneous Universe, and, again, local measurements are not very constraining. In addition, in void models, the presence of cosmological-scale adiabatic (curvature) inhomogeneity of mysterious origin suggests that we should also consider the possibility of isocurvature inhomogeneity between baryons and dark matter, in the form of an r -dependent f_b [55]. Thus, recalling that in our calculations we have used the CMB-based value $f_b = 0.168$ [32], our poor knowledge of the local baryon fraction in the context of LTB cosmologies will result in considerable further uncertainty in the kSZ power calculations presented here.

B. Small-scale baryonic astrophysics

Recall from figure 4 that, for the large ℓ 's which provide the strongest constraints on void models, the dominant length scales sourcing the kSZ in the fiducial model are very small, namely less than a Mpc. Matter perturbations on such small scales are expected to be strongly nonlinear, as we have already seen in section III when comparing the kSZ power calculated for linear and nonlinear matter power spectra. However, when we began the derivation of the kSZ effect, we assumed that the free electron fluctuations match those of the total matter, so that $\delta\rho_e/\rho_e = \delta\rho_m/\rho_m$. In the nonlinear regime, the baryonic (and hence electron) fluctuations are expected to be suppressed with respect to the total (or dark) matter power, due to interactions that become important on small scales (e.g., see [56]). Therefore, we expect the kSZ power sourced at these scales to be somewhat smaller than the calculations thus far (which used the standard Λ FLRW *total* matter power spectra) have indicated. To help examine the importance of this effect, it will be useful to consider the dependence of the sourcing length scales on the various model parameters.

In figure 8 we illustrate the dependence on the width and depth of the void of the wave number providing the peak contribution to the $\ell = 3000$ kSZ power, again for the fiducial profile and $h_0 = 0.71$. (The plotted peak wave number maximizes $d\mathcal{D}_\ell/d\ln k$, given in (34).) As we did for figure 4, we here plot the k scale that we would *conclude* sources the kSZ, if we mistakenly assumed that the correct model was standard Λ FLRW, when actually the (fiducial) void model was correct. This effective

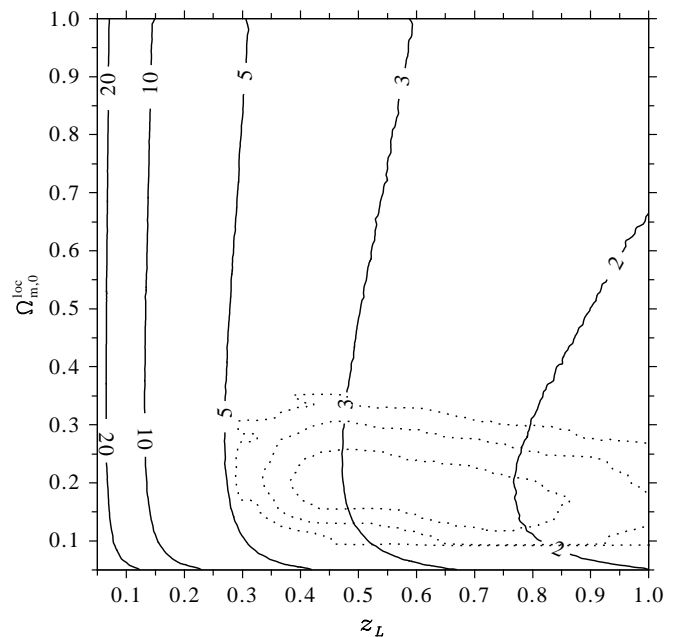


FIG. 8: Solid contours are the peak wave number contributing to the kSZ power at $\ell = 3000$, calculated in the Limber approximation using the Halofit nonlinear power, as a function of central matter density parameter, $\Omega_{m,0}^{\text{loc}}$, and a measure of the width of the void, z_L . The contour values are the peak scale k^Λ/h_0 (in Mpc^{-1}), calculated as described in section II B, and measured as a proper wave number today. Results are presented for the fiducial LTB profile with $h_0 = 0.71$. Dotted contours are the 1, 2, and 3 σ confidence levels from the SN data, which used the HST prior of $h_0 = 0.72 \pm 0.08$.

Λ FLRW scale is calculated according to the prescription of section II B. Figure 8 shows that the peak k scale generally increases as the void width decreases. This can be understood simply from the geometrical relation (21): keeping ℓ (or the angular scale) fixed, the relevant k scale must be inversely proportional to z , since $d_A(z) \propto z$, for sufficiently small redshift. This simple relationship is modified for large z or very deep voids, since relativistic effects then become important.

For the entire region of parameter space illustrated in figure 8, the peak scale is smaller than 1 Mpc^{-1} , and for the narrowest voids consistent with the SN constraints from section IV, namely $z_L \simeq 0.35$ at 2σ , the peak scale is $k^\Lambda/h_0 \simeq 4 \text{ Mpc}^{-1}$. On such small scales, hydrodynamical simulations indicate considerable suppression of baryon power with respect to dark matter power, although the various studies differ quantitatively in their predictions (e.g., see [56, 57]). Observations, on the other hand, most directly probe either the galaxy or the total matter power, rather than the baryon power. Therefore, it is clear that the poorly understood details of small-scale baryonic astrophysics add further considerable uncertainty to our estimates of kSZ power, although in this case we can say that our calculations will *overestimate* the kSZ for large ℓ 's. It is also clear that the models most

likely to avoid producing too much kSZ power will be the narrowest profiles consistent with the SN data: narrower profiles both produce less kSZ power when baryon suppression is ignored, and also result in greater baryon suppression, since the relevant length scales are the smallest.

VI. IMPORTANCE OF THE CONSISTENT LTB FRAMEWORK

At first glance, the kSZ power values in the z_L - $\Omega_{m,0}^{\text{loc}}$ plane presented in figure 6 appear remarkably similar to those of ZS10, considering the fully relativistic treatment of the background and the detailed treatment of the k scales performed here. However, note that for generic void profiles there is considerable arbitrariness in attempting to define an “edge”, with corresponding redshift z_L . Therefore, we only expect plots of this kind for different profiles to agree up to a scaling of the z_L axis by a factor of roughly unity. Considering the strong sensitivity of kSZ power to z_L exhibited in figure 6, this arbitrariness means that we can only say that our kSZ values are in agreement with those of ZS10 to within roughly an order of magnitude. This point is particularly relevant considering how different our smooth, polynomial fiducial LTB profile is from the “step function” Hubble bubble profile used in ZS10.

While we cannot state how precisely our kSZ power values agree with those of ZS10, we *can* directly compare our kSZ values for models which satisfy the SN constraints. Superimposed on figure 6 are the 1, 2, and 3σ confidence levels from the Union2 SN data calculated in section IV. Comparing these contours with those in ZS10, we can see that the kSZ power values for models which satisfy the SN constraints at 2σ are roughly *one tenth* those found in ZS10. A related observation is that ZS10 quote a minimum χ^2 of 605.4 for their void models with respect to the 557 Union2 SNe, which represents a much worse fit than our best-fit value of $\chi^2 = 539$. We believe that the poor fit of the ZS10 profiles to the SNe accounts for most of the roughly tenfold difference in our results. This illustrates the importance of performing the kSZ calculations within a consistent, LTB framework, with smooth radial profiles which provide a good fit to the SNe. To obtain meaningful estimates of the kSZ power in void models, we cannot rely on void profiles which provide a poor fit to the SNe.

We can reinforce this point by calculating a quantity related to, but distinct from, the kSZ power, namely the Compton y -distortion of the CMB frequency spectrum. This distortion arises from the scattering of CMB photons from inside our past light cone into our line of sight, and has been used to provide constraints on void models [19, 58, 59]. Like the kSZ effect, the y -distortion also depends on the dipole $\beta(z)$ along our past light cone, but is a background-level effect, so is independent of the matter power spectrum. In the single-scattering and linear approximations, and when the dipole anisotropy domi-

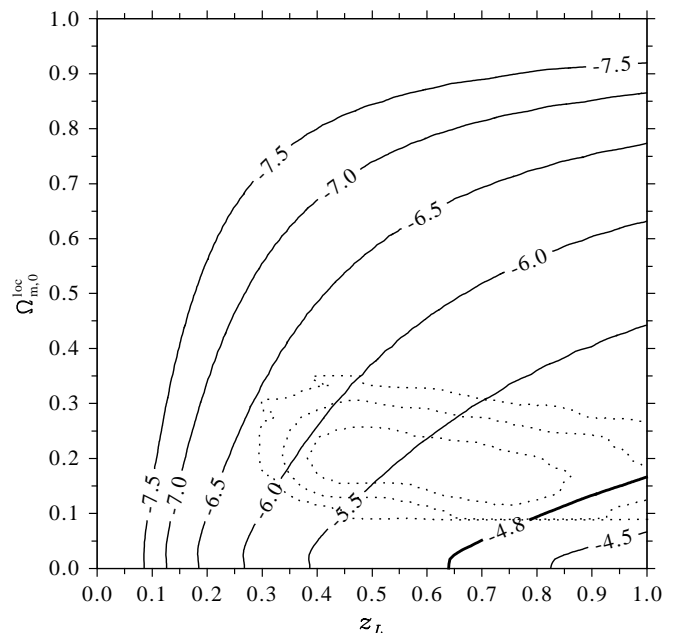


FIG. 9: Solid contours are the y -distortion, as a function of central matter density parameter, $\Omega_{m,0}^{\text{loc}}$, and a measure of the width of the void, z_L . The contour values are $\log_{10} y$, calculated using (40), and the heavy contour represents the COBE upper limit of $y < 1.5 \times 10^{-5}$ [60]. Results are presented for the fiducial LTB profile with $h_0 = 0.71$. Dotted contours are the 1, 2, and 3σ confidence levels from the SN data, which used the HST prior of $h_0 = 0.72 \pm 0.08$.

nates, the y -distortion can be written as [19]

$$y = \frac{7}{10} \int_0^{r_{\text{re}}} dr \frac{d\tau}{dz} \frac{dz}{dr} \beta(r)^2 = \frac{7}{10} \int_0^{r_{\text{re}}} dr F(r) \beta(r), \quad (40)$$

where r_{re} is the radial coordinate of (the assumed abrupt) reionization.

The similarity of expression (40) to expression (30) for the kSZ power in the Limber approximation means that we can readily calculate the y -distortion for our fiducial profile. In figure 9 we plot the y -distortion in the z_L - $\Omega_{m,0}^{\text{loc}}$ plane for the fiducial LTB profile. The heavy contour indicates the 2σ upper limit of $y < 1.5 \times 10^{-5}$ from the COBE satellite [60]. Superimposed on the figure are our 1, 2, and 3σ confidence levels from the Union2 SN data. It is apparent that almost all of the models allowed by the SN data have y -distortion values below the COBE limit, and hence the y -distortion provides no significant constraint on void models.

This result is in sharp contrast to [59], who found that almost all models allowed by SN data were *above* the COBE limit, and hence ruled out. Importantly, the void models used in [59] were the same Hubble bubble models as were studied in ZS10. The simplicity of the y -distortion calculation means that it is free of the ambiguities of harmonic decomposition, k scales, and small-scale baryonic astrophysics which plague the kSZ calculation.

Therefore, this result demonstrates again that the treatment of the background spacetime, and, in particular, obtaining good fits to the SN data, is crucial in obtaining meaningful constraints on void models for acceleration.

VII. CONCLUSIONS

Our results indicate that void models which satisfy local constraints on the Hubble rate and fit the SN observations predict considerably higher kSZ power for $\ell \simeq 2000$ – 3000 than the *total* anisotropy power observed at those scales by SPT and ACT. Thus all local void models would appear to be ruled out. To evade these high- ℓ constraints, the kSZ power would need to be reduced by a factor of roughly 30 for the narrowest voids allowed by the SN data, with our conservative interpretation of the power measurements. We have highlighted several caveats and ambiguities that render our calculations uncertain and could in principle lead to such a reduction. By way of summary, we list them here:

- (1) We have needed a harmonic decomposition of the matter fluctuations, although it is unclear how this should be done at late times on an LTB background.
- (2) We have attempted to match the late time matter power in the LTB model to that in standard Λ FLRW via the physically correct prescription, but we have found that it is not possible to do this without ambiguity in the k scales and hence in the matter power.
- (3) We have assumed that the linear kSZ contribution $\int \delta\beta d\tau$ vanishes in LTB models as it does in FLRW, although this would need to be checked explicitly with a proper LTB perturbation formalism.
- (4) The kSZ power is very sensitive to the parameters σ_8 and f_b , but their *local* values are very uncertain, both theoretically and observationally.
- (5) We have shown that the kSZ power for large ℓ is sourced mainly by very small scales, between 1 and 0.1 Mpc. The baryon power is expected to be suppressed significantly relative to total matter power on these scales, reducing the kSZ power by an uncertain amount.
- (6) The strong sensitivity of kSZ power to void width means that model dependence in the SN data, or simply changes to the void radial profile, may substantially affect the kSZ power.
- (7) It is likely that the dipole values along the light cone, and hence the kSZ power, could be reduced by choosing an appropriate isocurvature profile between radiation and matter at early times [25, 55], although it is likely that this would entail fine tuning.

- (8) It is also possible that including a significant late-time LTB decaying mode could evade the kSZ constraints, although this would entail a drastic departure from the standard view of the early Universe.

To determine the importance of the first three points listed above would require a proper treatment of perturbations on LTB backgrounds. To reduce the uncertainty due to points (4) and (5) would require a direct measurement of the *baryon* power spectrum on $\sim 1/3$ Mpc scales, as well as a measurement of the baryon fraction, both at redshifts $z \simeq 0.5$. It is clear, though, that a void must be as narrow as possible if it is to minimize the kSZ power.

Our result that void models with the fiducial parameters predict, at 2σ confidence, at least a factor of roughly 30 larger kSZ power than that observed is considerably weaker than the corresponding result of ZS10, who found a discrepancy of more than three orders of magnitude for voids that fit the SNe at 2σ confidence. The difference between our results is presumably mainly due to our rigorous LTB treatment of the background together with our careful treatment of wave numbers. Our more conservative interpretation of the SPT and ACT power measurements also contributes to the difference in our results. This conclusion is reinforced by the y -distortion values for our models, which are strongly at odds with those of [59], who also used a simple Hubble bubble model. Again, this emphasizes the importance of using smooth radial profiles which fit the SN data well in order to obtain meaningful constraints on void models.

As we stressed in the [Introduction](#), if a void model is to generate the observed primary CMB anisotropies, it must have a *local* Hubble rate low enough ($h_0 \simeq 0.45$) to rule out all such models [16, 19, 20]. This conclusion is independent of the poorly understood details of the IC's or evolution of perturbations on LTB backgrounds, and it is insensitive to the uncertainties of small-scale baryonic astrophysics as well as to the values of locally poorly determined parameters such as σ_8 and f_b . For growing mode LTB profiles, the only chance to avoid this CMB constraint is possibly by substantially altering the primordial spectrum from scale invariance [19]. But it is not enough, of course, to simply introduce a significant non-scale-invariant feature: that feature must be just so contrived that together with the local void profile it *mimics* the near-scale-invariant spectrum expected in the standard Λ FLRW model! In [44], e.g., a five-parameter modification of the primordial spectrum was required in order to match only the WMAP CMB data (no small-scale CMB data was used), with the somewhat improved local Hubble rate of $h_0 \simeq 0.60$. The effect of an early radiation inhomogeneity [55] should be negligible at late times [19], and hence it appears unlikely that this could provide a loophole.

The superb sensitivity of the linear kSZ approach goes a very substantial way towards closing the rather contrived loophole of modifying the primordial spectrum for void models. However, the various ambiguities in its application to void models should be considerably less im-

portant in a related but distinct application: constraining departures from homogeneity within the standard Λ FLRW framework. That is, *assuming* that the background is near-FLRW with the usual fraction of dark energy, and that the parameters σ_8 and f_b are as indicated by the CMB, we can use the linear kSZ effect to constrain small departures from homogeneity, as done in ZS10. Also, at greater redshifts, the length scales sourcing the kSZ at fixed ℓ will be larger, reducing the uncertainty in baryonic astrophysics. Thus the linear kSZ effect should bring us closer to observationally confirming the long-held belief in cosmological homogeneity.

Acknowledgments

We thank Douglas Scott and Albert Stebbins for useful discussions. This research was supported by the Canadian Space Agency.

Appendix: The Lemaître-Tolman-Bondi solution

We model the Universe at background level as a spherically symmetric distribution of pressureless matter, with the observer at the centre. For this spacetime, Einstein's equations can be solved exactly, resulting in the LTB solution. The metric can be written

$$ds^2 = -dt^2 + \frac{Y'^2}{1-K} dr^2 + Y^2 d\Omega^2, \quad (\text{A.1})$$

where a prime denotes the derivative with respect to comoving radial coordinate r , and t is the proper time along the comoving worldlines. The function $K = K(r)$ is arbitrary, and the areal radius $Y = Y(t, r)$ is given parametrically by

$$Y = \begin{cases} \frac{M}{K}(1 - \cosh \eta) & K < 0, \\ \frac{M}{K}(1 - \cos \eta) & 0 < K < 1, \\ \left(\frac{9M}{2}\right)^{1/3} (t - t_B)^{2/3} & K = 0, \end{cases} \quad (\text{A.2})$$

$$t - t_B = \begin{cases} \frac{M}{(-K)^{3/2}}(\sinh \eta - \eta) & K < 0, \\ \frac{M}{K^{3/2}}(\eta - \sin \eta) & 0 < K < 1. \end{cases} \quad (\text{A.3})$$

This exact solution reveals the presence of a second free radial function, $t_B = t_B(r)$, which is known as the “bang time” function, since the cosmological singularity occurs

at $t = t_B(r)$. Throughout this work we assume a homogeneous big bang and set $t_B = 0$. In this case the LTB solution contains no decaying mode [17, 61], and hence we retain the standard inflationary picture of an essentially homogeneous early (but post-inflation) Universe. There is also a third free radial function, $M(r)$, which we set to $M(r) = r^3$ without loss of generality as our gauge condition.

The radial and transverse comoving expansion rates are given by $H_{\parallel} = \dot{Y}/Y'$ and $H_{\perp} = \dot{Y}/Y$, respectively, where the overdot denotes the derivative with respect to t . We define the local density parameter by $\Omega_m^{\text{loc}} \equiv 24\pi G \rho_m / \theta^2$, where ρ_m is the *total* matter density and θ the comoving volume expansion. At the centre of symmetry in an arbitrary LTB spacetime, we have $H_{\parallel} = H_{\perp} \equiv H$. The angular diameter distance from the centre to redshift z is simply $d_A = Y(z)$.

The LTB spacetime is completely determined once the single free radial profile $K(r)$ is specified. Based on our previous experience with a wide range of LTB profiles [16, 19], we chose for this study a simple profile which depends on only two parameters, a width and a depth. Explicitly, we chose

$$K(r) = \begin{cases} K_0 \left[\left(\frac{r}{L}\right)^5 - \frac{9}{5} \left(\frac{r}{L}\right)^4 + \left(\frac{r}{L}\right)^2 \right] & r \leq L, \\ \frac{K_0 L}{5} \frac{1}{r} & r > L. \end{cases} \quad (\text{A.4})$$

The profile width and depth are determined by the parameters L and K_0 , respectively, but it is normally more physically relevant to specify the parameter $\Omega_{m,0}^{\text{loc}} \equiv \Omega_m^{\text{loc}}(z = 0)$ at the observation point to characterize the depth, and to specify the redshift $z_L \equiv z(r = L)$ to determine the width. Finally, the observation point is determined by the corresponding proper time coordinate, t_0 , or, more observationally relevantly, the Hubble rate today at the centre, $H_0 \equiv H(t_0)$. We will refer to the general profile, (A.4), with unspecified K_0 , L , and H_0 , as the *fiducial profile*. The model with the specific values $\Omega_{m,0}^{\text{loc}} = 0.2$, $z_L = 0.5$, and $h_0 = 0.71$ (where $H_0 \equiv 100 h_0 \text{ km s}^{-1} \text{ Mpc}^{-1}$) will be referred to as the *fiducial model*; as shown in section IV, this model is a very good fit to the supernova data. In all of our calculations we chose the values $f_b = 0.168$ and $\sigma_8 = 0.81$ for the baryon fraction and matter amplitude today, as CMB observations suggest [32] in the context of FLRW models. In our numerical code, we check for the presence of shell crossing singularities along the past light cone, and exclude any models which exhibit them, since the LTB solution is not valid in such a case. Further details and a discussion of our numerical implementation are provided in [19].

[1] S. Perlmutter and B. P. Schmidt, Lect. Notes Phys. **598**, 195 (2003), arXiv:astro-ph/0303428.

[2] J. Frieman, M. Turner, and D. Huterer, Ann. Rev. As-

- tron. Astrophys. **46**, 385 (2008), arXiv:0803.0982 [astro-ph].
- [3] E. V. Linder, Rept. Prog. Phys. **71**, 056901 (2008), arXiv:0801.2968 [astro-ph].
- [4] K. Tomita, Astrophys. J. **529**, 38 (2000), arXiv:astro-ph/9906027.
- [5] S. P. Goodwin, P. A. Thomas, A. J. Barber, J. Gribbin, and L. I. Onuora (1999), arXiv:astro-ph/9906187.
- [6] M.-N. Celerier, Astron. Astrophys. **353**, 63 (2000), arXiv:astro-ph/9907206.
- [7] J. W. Moffat and D. C. Tatarski, Astrophys. J. **453**, 17 (1995), arXiv:astro-ph/9407036.
- [8] K.-i. Nakao et al., Astrophys. J. **453**, 541 (1995), arXiv:astro-ph/9502054.
- [9] K. Tomita, Astrophys. J. **461**, 507 (1996).
- [10] N. P. Humphreys, R. Maartens, and D. R. Matraers, Astrophys. J. **477**, 47 (1997), arXiv:astro-ph/9602033.
- [11] S. Foreman, A. Moss, J. P. Zibin, and D. Scott, Phys. Rev. **D82**, 103532 (2010), arXiv:1009.0273 [astro-ph.CO].
- [12] V. Marra and A. Notari (2011), arXiv:1102.1015 [astro-ph.CO].
- [13] K. Bolejko, M.-N. Celerier, and A. Krasinski (2011), arXiv:1102.1449 [astro-ph.CO].
- [14] C.-M. Yoo, T. Kai, and K.-i. Nakao, Prog. Theor. Phys. **120**, 937 (2008), arXiv:0807.0932 [astro-ph].
- [15] J. Garcia-Bellido and T. Haugboelle, JCAP **0804**, 003 (2008), arXiv:0802.1523 [astro-ph].
- [16] J. P. Zibin, A. Moss, and D. Scott, Phys. Rev. Lett. **101**, 251303 (2008), arXiv:0809.3761 [astro-ph].
- [17] J. P. Zibin, Phys. Rev. **D78**, 043504 (2008), arXiv:0804.1787 [astro-ph].
- [18] C. Clarkson, T. Clifton, and S. February, JCAP **0906**, 025 (2009), arXiv:0903.5040 [astro-ph.CO].
- [19] A. Moss, J. P. Zibin, and D. Scott, Phys. Rev. **D83**, 103515 (2011), arXiv:1007.3725 [astro-ph.CO].
- [20] T. Biswas, A. Notari, and W. Valkenburg, JCAP **1011**, 030 (2010), arXiv:1007.3065 [astro-ph.CO].
- [21] V. Marra and M. Paakkonen, JCAP **1012**, 021 (2010), arXiv:1009.4193 [astro-ph.CO].
- [22] R. A. Sunyaev and Y. B. Zeldovich, Mon. Not. Roy. Astron. Soc. **190**, 413 (1980).
- [23] R. A. Vanderveld, E. E. Flanagan, and I. Wasserman, Phys. Rev. **D74**, 023506 (2006), arXiv:astro-ph/0602476.
- [24] J. Garcia-Bellido and T. Haugboelle, JCAP **0809**, 016 (2008), arXiv:0807.1326 [astro-ph].
- [25] C.-M. Yoo, K.-i. Nakao, and M. Sasaki, JCAP **1010**, 011 (2010), arXiv:1008.0469 [astro-ph.CO].
- [26] P. Zhang and A. Stebbins (2010), arXiv:1009.3967 [astro-ph.CO].
- [27] G. Lemaître, Ann. Soc. Sci. Bruxelles **53**, 51 (1933).
- [28] R. C. Tolman, Proc. Nat. Acad. Sci. **20**, 169 (1934).
- [29] H. Bondi, Mon. Not. Roy. Astron. Soc. **107**, 410 (1947).
- [30] N. Kaiser, Astrophys. J. **282**, 374 (1984).
- [31] J. P. Ostriker and E. T. Vishniac, Astrophys. J. Lett. **306**, L51 (1986).
- [32] D. Larson et al., Astrophys. J. Suppl. **192**, 16 (2011), arXiv:1001.4635 [astro-ph.CO].
- [33] D. J. Eisenstein et al. (SDSS), Astrophys. J. **633**, 560 (2005), arXiv:astro-ph/0501171.
- [34] T. Wickramasinghe and T. N. Ukwatta, Mon. Not. Roy. Astron. Soc. **406**, 548 (2010), arXiv:1003.0483 [astro-ph.CO].
- [35] A. Lewis, A. Challinor, and A. Lasenby, Astrophys. J. **538**, 473 (2000), arXiv:astro-ph/9911177.
- [36] R. E. Smith et al. (The Virgo Consortium), Mon. Not. Roy. Astron. Soc. **341**, 1311 (2003), arXiv:astro-ph/0207664.
- [37] N. Mustapha, B. A. Bassett, C. Hellaby, and G. F. R. Ellis, Class. Quant. Grav. **15**, 2363 (1998), arXiv:gr-qc/9708043.
- [38] D. N. Limber, Astrophys. J. **117**, 134 (1953).
- [39] N. Afshordi, Y.-S. Loh, and M. A. Strauss, Phys. Rev. **D69**, 083524 (2004), arXiv:astro-ph/0308260.
- [40] R. Amanullah et al., Astrophys. J. **716**, 712 (2010), arXiv:1004.1711 [astro-ph.CO].
- [41] W. L. Freedman et al. (HST), Astrophys. J. **553**, 47 (2001), arXiv:astro-ph/0012376.
- [42] A. G. Riess et al., Astrophys. J. **699**, 539 (2009), arXiv:0905.0695 [astro-ph.CO].
- [43] A. G. Riess et al., Astrophys. J. **730**, 119 (2011), arXiv:1103.2976 [astro-ph.CO].
- [44] S. Nadathur and S. Sarkar, Phys. Rev. **D83**, 063506 (2011), arXiv:1012.3460 [astro-ph.CO].
- [45] A. Lewis and S. Bridle, Phys. Rev. **D66**, 103511 (2002), arXiv:astro-ph/0205436.
- [46] R. G. Carlberg et al. (1997), arXiv:astro-ph/9711272.
- [47] M. Fukugita, C. J. Hogan, and P. J. E. Peebles, Astrophys. J. **503**, 518 (1998), arXiv:astro-ph/9712020.
- [48] C. L. Reichardt et al., Astrophys. J. **694**, 1200 (2009), arXiv:0801.1491 [astro-ph].
- [49] N. R. Hall et al., Astrophys. J. **718**, 632 (2010), arXiv:0912.4315 [astro-ph.CO].
- [50] E. Shirokoff et al., Astrophys. J. **736**, 61 (2011), arXiv:1012.4788 [astro-ph.CO].
- [51] S. Das et al., Astrophys. J. **729**, 62 (2011), arXiv:1009.0847 [astro-ph.CO].
- [52] H. Alnes and M. Amarzguoui, Phys. Rev. **D74**, 103520 (2006), arXiv:astro-ph/0607334.
- [53] O. Dore, J. F. Hennawi, and D. N. Spergel, Astrophys. J. **606**, 46 (2004), arXiv:astro-ph/0309337.
- [54] L. Fu et al., Astron. Astrophys. **479**, 9 (2008), arXiv:0712.0884 [astro-ph].
- [55] C. Clarkson and M. Regis, JCAP **1102**, 013 (2011), arXiv:1007.3443 [astro-ph.CO].
- [56] Y. P. Jing, P. Zhang, W. P. Lin, L. Gao, and V. Springel, Astrophys. J. **640**, L119 (2006), arXiv:astro-ph/0512426.
- [57] S. DeDeo, D. N. Spergel, and H. Trac (2005), arXiv:astro-ph/0511060.
- [58] J. Goodman, Phys. Rev. **D52**, 1821 (1995), arXiv:astro-ph/9506068.
- [59] R. R. Caldwell and A. Stebbins, Phys. Rev. Lett. **100**, 191302 (2008), arXiv:0711.3459 [astro-ph].
- [60] D. J. Fixsen et al., Astrophys. J. **473**, 576 (1996), arXiv:astro-ph/9605054.
- [61] J. Silk, Astron. Astrophys. **59**, 53 (1977).